# Structure and shape transformation from multiply twinned particles to epitaxial nanocrystals: Importance of interface on the structure of Ag nanoparticles

B. Q. Li and J. M. Zuo
*Department of Materials Science and Engineering and Frederick Seitz Materials Research Laboratory, University of Illinois, Urbana, Illinois 61801, USA*
(Received 17 December 2004; revised manuscript received 3 May 2005; published 16 August 2005)

The effect of a substrate on the structure of nanometer-sized metal particles was investigated for Ag on silicon surfaces by using high-resolution transmission electron microscope and electron diffraction. The nanometer-sized Ag particles, formed by the vapor deposition of Ag on (001) hydrogen-terminated Si (H-Si) surfaces at room temperature, adopt multiply twinned structures. Upon annealing, the multiply twinned Ag nanoparticles on H-Si (001) transform into fcc nanocrystals. The fcc Ag takes up the cube-on-cube epitaxy, with the orientation relationship of Ag(001)//Si(001) and Ag [110]//Si [110]. An energetic model is developed to account for the structure and shape transition of supported multiply twinned particles to fcc epitaxial nanocrystals. Possible transition mechanisms are discussed.

DOI: 10.1103/PhysRevB.72.085434 PACS number(s): 61.46.+w, 68.35.−p, 68.55.Jk, 68.37.Lp

## I. INTRODUCTION

At the nanoscale, the structure and shape of a particle on a substrate is remarkably sensitive to the particle-substrate interaction. An extreme example is the spontaneous formation of ordered nanostructures in mismatched heteroepitaxial semiconductor systems due to the elastic interaction.[1] For nanoparticles of noble and transition metals, early studies of thin-film growth revealed substrate-dependent multiply twinned particle formation.[2–4] More recent studies have focused on free particles and results have shown size-dependent icosahedral and decahedral multiply twinned structures with the fivefold symmetry.[5,6] Direct experimental evidence of different particle structures comes mostly from electron imaging and diffraction.[7–12] However, most high-resolution electron microscopy (HREM) observations are made for particles supported on surfaces, in which case the role of the substrate on the particle structure and the structural transition is generally unknown.[5,13] Nanoparticle-substrate interaction is an important issue because metallic particles used in applications, such as heterogeneous catalyst and magnetic recording media, are supported on certain substrates. It is also an important surface science issue since nanoparticle structures at the early stage of growth have a large effect on thin-film microstructure as we show here.

In this paper, we report an experimental study of the structure and transition of Ag nanoparticles on hydrogen-terminated Si (H-Si) (001) surfaces using electron diffraction and high-resolution electron imaging. We show that Ag multiply twinned particles (MTPs) form on H-Si (001) surfaces. Upon annealing, the MTPs transform into fcc nanocrystals with the cube-on-cube epitaxy relative to the Si (001). The transformation depends on both annealing temperature and particle size. The growth is in sharp contrast to Ag on the clean Si (001)-$2\times1$ surface, where the Stranski-Krastanov growth mode is observed. At room temperature, the wetting layer terminates at about 1 ML (monolayer) and epitaxial three-dimensional (3D) islands form on the wetting layer.[14–17] The growth behavior is also very different from that on H-Si (111) surfaces, where fcc Ag nanocrystals dominate from the early stages of growth and increasing Ag nanocrystal size leads to improved coincident-site-lattice (CSL) heteroepitaxy.[18,19] We explain the difference in growth based on the particle-substrate interaction and the driving force for particle structural transition. The results here show the significance of a nanoparticle-substrate interface on a particle structure and the orientation in additional to the particle size.

## II. EXPERIMENT

The growth and subsequent annealing of Ag nanoparticles were carried out in an UHV transmission electron microscope (base pressure $2\times10^{-10}$ Torr), which is described in detail elsewhere.[20] Si (001) and Si (111) (phosphorus-doped, resistivity about 9 $\Omega$ cm, $15\times6$ mm$^2$ substrates were initially backthinned by grinding, followed by the chemical etching for electron transparency. After degreasing and chemical cleaning, the samples were etched in a 40% $NH_4F$ solution, followed by a short rinse in de-ionized water. The chemically prepared H-terminated samples were then transferred to the UHV chamber. Ag was deposited using an Omicron EFM3 electron-beam evaporator. The growth rate was about 0.5 ML/min, calibrated by *in situ* Auger electron spectroscopy and *ex situ* Rutherford backscattering spectroscopy measurements. After deposition, the samples were annealed *in situ* by direct current heating. The temperature was calibrated with a thermocouple in a prior experiment.

HREM observations were carried out *ex situ* using a JEOL 2010 field emission gun electron microscope, operated at 200 kV. All images were recorded digitally using a slow-scan charge coupled device camera. Transmission electron diffraction patterns were recorded on image plates to facilitate quantitative analysis. The nanoarea electron diffraction technique[21] was extensively employed to obtain higher beam intensity, especially in the case of lower Ag coverage. The samples were briefly exposed to atmosphere during the transfer from the UHV transmission electron microscope (TEM) to the JEOL 2010F TEM. To investigate the effect of this

 

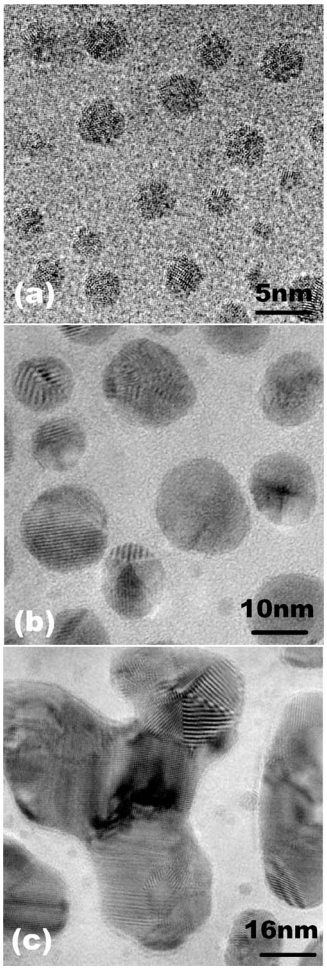


FIG. 1. The structural evolution of Ag particles grown on H-Si (001) surfaces at room temperature. The Ag coverage is 4, 20, and 60 ML, respectively. The high-resolution images were taken near the Si [001] zone axis. At 4 ML coverage, most Ag particles adopt MTP morphology [Fig. 1(a)]. Figures 1(b) and 1(c) show the particle morphology at 20 and 60 ML coverages.

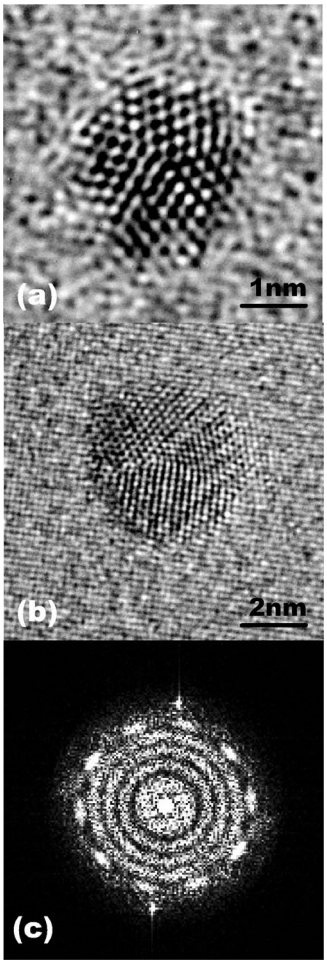


FIG. 2. (a) and (b) show two typical MTPs in their fivefold orientation and (c) is Fourier transformation of (a).

short exposure, we have compared the *in situ* electron diffraction patterns obtained in the UHV TEM and the ones obtained in the 2010F TEM in prior experiments, and found no appreciable difference. Also no evidence of Ag oxidation was found.

## III. RESULTS AND DISCUSSION

Figure 1 illustrates the structural evolution of Ag nanoparticles grown on H-Si (001) surfaces at room temperature. The high-resolution images were taken near the Si [001] zone axis with Ag coverage at 4, 20, and 60 ML, respectively. At 4 ML coverage, most Ag particles adopt MTP morphology [Fig. 1(a)]. Figures 2(a) and 2(b) show two typical MTPs in their fivefold orientation, as evidenced by the fivefold symmetry of the corresponding Fourier transformation in Figure 2(c). The diameters of the particles are 2.5 and 5 nm, respectively. The MTP morphology persists at 8 ML. Figure 1(b) shows the particle morphology at 20 ML coverage. The average size of Ag particles increases with the Ag coverage, from 2.7 nm at 4 ML to 14 nm at 20 ML, with 3.7 nm for 8 ML in between.A further increase in coverage leads to particle coalescence. At 60 ML coverage, fractal islands are formed with complex microstructure [Fig. 1(c)].

In comparison, our previous study showed that the Ag particles on H-Si (111) have drastically different morphologies.[18,19] Figures 3(a)–3(c) display the high-resolution images of Ag particles deposited at the same conditions on H-Si (111) at the coverage of 4, 20, and 60 ML, respectively. The images were taken close to the Si (111) zone axis. Multiply twinned particles are rarely observed on the HSi (111) surfaces. Most Ag particles at 4 ML coverage have single set of Moire fringes although the fringes are not perfectly aligned to the Si (220) plane. This suggests that fcc Ag nanocrystals dominate from the early stage of Ag particle growth on H-Si (111). Coalescence sets in at 20 ML [Fig. 3(b)], and percolated Ag films with domains of different fcc stacking are formed at 60 ML [Fig. 3(c). The film is epitaxial, in contrast to the Ag on H-Si (001), where the film is polycrystalline without a fixed epitaxial relationship. Thus, compared to the case on Si (111), the stabilization of large MTPs on H-Si (001) leads to a significantly different microstructural evolution during thin film growth.

The difference in nanoparticle structure on H-Si (001) and H-Si (111) is related to the formation mechanism of the Ag

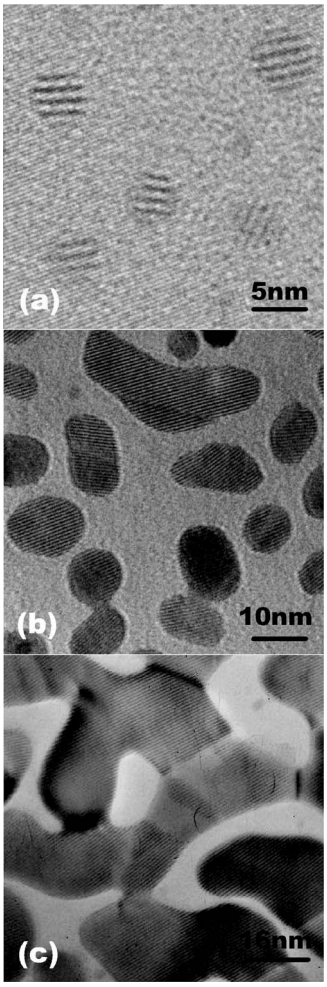


FIG. 3. Electron images of Ag growth on H-Si (111) at the coverage of (a) 4, (b) 20, and (c) 60 ML, respectively. The images were taken close to the Si [111] zone axis. The Ag growth condition was same as that of Fig. 1.

MTPs and the role the substrates playing in the process. The growth mechanism of MTPs has been debated for a long time since the discovery of the multiply twinned particles.[1,2,4] Allpress and Sanders[2] suggested that they are due to the high incidence of twinning during growth. Ino[4] argued that they are intrinsic equilibrium structures of lower energy at smaller sizes. Bauer *et al.*[22] proposed that MTPs are the result of coalescence of small particles. Gillet[23] suggested that they grow by layer growth around the fivefold axis and thus a kinetic phenomenon. Our results presented here highlight the importance of interface structure in determining the particle structures.

Ag particles have a strong tendency to grow with {111} (the dense packing plane) parallel to the substrate. When grown on the H-Si (111) substrate, which also has the hexagonal lattice, Ag particles have two equally probable orientations, or double positioning.[24] Ag (111) planes preferably align to the H-Si (111) substrate. Every four Ag atoms match with three Si atoms, forming a coincident-site lattice at the interface. This minimizes the interface energy,[18] and potentially suppresses the formation of Ag MTPs on the H-Si (111) surface. In contrast, multiple or random positioning is pronounced for Ag on H-Si (001). Since the H-Si (001) surface has a fourfold symmetry, a Ag (111) particle with threefold symmetry can be oriented with two pairs of four orientations simultaneously, distributed in a random manner. The multiple orientations and deviations from the ideal orientation presented in small particles,[25] result in diffraction patterns with rings and arcs, which will be discussed in the next paragraph. Because Ag-Ag interaction is much stronger than that between Ag and the H-Si (001) substrate, we expect an initial tetrahedral cluster with Ag (111) paralleling to the substrate. The tetrahedron will grow by incorporating impinging Ag adatoms from the deposition flux and those that initially land on the substrate and subsequently upward diffuse to the tetrahedron surface.[26] At a certain stage, the coalescence of tetrahedral clusters is expected, resulting in the formation of multiply twinned icosahedra or decahedra.[22] The other scenario is due to atomic attachments. There is more than one way to attach Ag adatoms to the cluster surface. Growth errors can also lead to the formation of MTPs.

Figure 4 shows the electron diffraction patterns of Ag particles on H-Si (001) at the coverage of 4, 8, and 20 ML, respectively, taken close to the Si [001] zone axis. The diffraction patterns consist of a continuous (111) ring and (002), (220), and (311) arcs. The continuous (111) ring, instead of the fivefold symmetry in Ag (111) reflection, as shown in Fig. 2, is due to the random positioning of the MTPs because of the weak interaction between Ag and H-Si (001), as discussed in the last paragraph. The Ag (002) arcs, which come from a small percentage of Ag particles with Ag (002) planes aligning to the Si (001) substrate, become narrower and stronger as the coverage increases. To compare with the electron diffraction patterns from unsupported silver particles,[27] we integrated the radial intensity of the diffraction patterns in Fig. 4(b) (8 ML). The radial intensity profile of the diffraction pattern from Fig. 4(b) is similar to the diffraction profiles from unsupported silver MTPs, The MTPs are randomly orientated as evidenced by the appearance of Ag (111), (002), (220), and (311) reflections. The broad scattering profile of silver particles, as opposed to sharp Bragg peaks, is due to the absence of long periodic order in the MTPs, as well as due to the small sizes of the Ag particles.

The multiply twinned structure of Ag particles and multiple Ag reflections from the Ag particles are also in sharp contrast to the Ag growth behavior on Si (001) surfaces, which has been extensively studied. Ag grows on Si(001) in the Stranski-Krastanov growth mode, where the wetting layer terminates at about 1 ML (monolayer) and epitaxial 3D islands with Ag(001)//Si(001) or Ag(111)//Si(001) are formed on the wetting layer.[14,17,28,29]

Significant structural changes in small particles were observed upon annealing. Figure 5 shows the HREM images of the samples of the as-deposited, annealed at 673 and 723 K. As discussed above, multiply twinned Ag particles dominate in the RT as-deposited sample at the coverage of 8 ML. Upon annealing, the average particle sizes in projection change slightly from 3.7 nm at RT to 4 nm at 673 K and 4.5 nm at 723 K (see the corresponding diameter histograms in Fig. 5). The particle density decreases as the annealing proceeds, varying from $2.37\times10^{12}\,\mathrm{cm}^{-2}$ at RT, $1.41\times10^{12}\,\mathrm{cm}^{-2}$ at 673 K for 2h, to $1.22\times10^{12}\,\mathrm{cm}^{-2}$ at

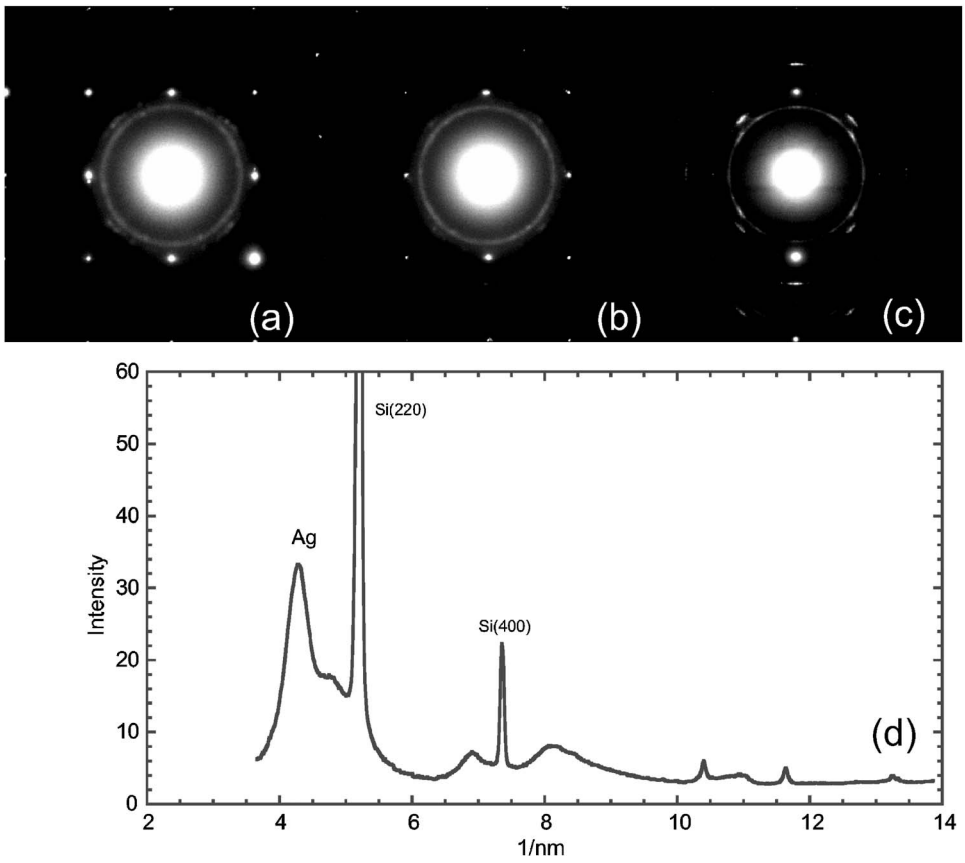


FIG. 4. Electron diffraction patterns, taken along the Si [001] zone axis, of Ag particles on H-Si (001) at the coverage of 4 (a), 8 (b), and 20 ML (c), respectively. (d) is the radial intensity profile of the diffraction pattern at 8 ML.

723 K for 2 h. Thus, some coarsening occurs during annealing.

More strikingly, some Ag particles transform from multiple twinned structures to epitaxial truncated pyramids [Figs. 5(b) and 5(c)]. At 673 K, about 30% particles are transformed. Most of these transformed particles are smaller ones, less than the average particle size of 4 nm. The transformation is more complete after annealing at 723 K. At this temperature, more than 80% are transformed. The remaining MTPs are significantly larger, usually greater than 6 nm in diameter.

Figure 6 shows the epitaxial relationship of Ag particles and the Si (001) substrate. The particle is a truncated pyramid, which is the fcc crystal on the Si (001) substrate with Ag(001)//Si(001) and Ag [110]//Si [110], as indicated by the diffraction in Fig. 5. By adopting a CSL interface[18,19] with every three Si atoms matching with four Ag atoms, the lattice mismatch is only about-0.3%. A few elongated islands are also observed, but they are not the energetically favorable shape from the standpoint of surface energy. The square or truncated pyramid shapes are further supported by the cross-shaped Ag (200) diffraction spots, which comes from the Fourier transformation of a rectangular shape.

The above results suggest that there must be an energy gain, which drives the transition from the Ag MTPs to the truncated pyramids to occur. For free Ag nanoparticles, it is known that icosahedra are favored at small sizes, decahedra at intermediate sizes, and fcc truncated octahedra at large sizes.[27] It is particularly interesting to notice that the particle sizes are in the same size range before and after the transition in the present experiment.

To understand the driving force for the transformation from MTPs to fcc truncated pyramids on the H-Si (001) surface, we first look at the energy of a multiple twinned particle. We use an icosahedron particle for analysis, however, the arguments apply equally for other types of MTPs. Assume the icosahedron with edge length $a$ and volume $V$ sitting on the H-Si (001) surface, as shown in Fig. 7. The icosahedron can be considered by assembling 20 single-crystal tetrahedra subunits bounded by (111) faces sharing one apex. The icosahedron is subject to substantial strains in order to fill the geometric gap left between the tetrahedra. By adopting the inhomogeneous strain model for the icosahedron,[30] the strain energy of the particle can be written as

$$E_{Ic}^{1} = \frac{2\mu\varepsilon_I^2}{9}\left(\frac{1+\nu}{1-\nu}\right)V, \tag{1}$$

where $\mu$ is the shear modulus, $\varepsilon_I$ is the strain in the particle, and $\nu$ is the Poisson's ratio.

The surface and interface energy of the icosahedron is given as

$$E_{Ic}^{2} = \frac{19\sqrt{3}a^2}{4}\gamma_{Ag(111)} + \frac{\sqrt{3}a^2}{4}(\gamma_I - \gamma_{H\text{-}Si(001)}), \tag{2}$$

where $\gamma_{111}$ is the Ag (111) surface energy density, $\gamma_I$ is the Ag and the H-Si (001) interfacial energy density, $\gamma_{H\text{-}Si(001)}$ is the surface energy density of the H-Si (001) surface, and $\sqrt{3}a^2/4$ is the area of the triangle face of the icosahedron.

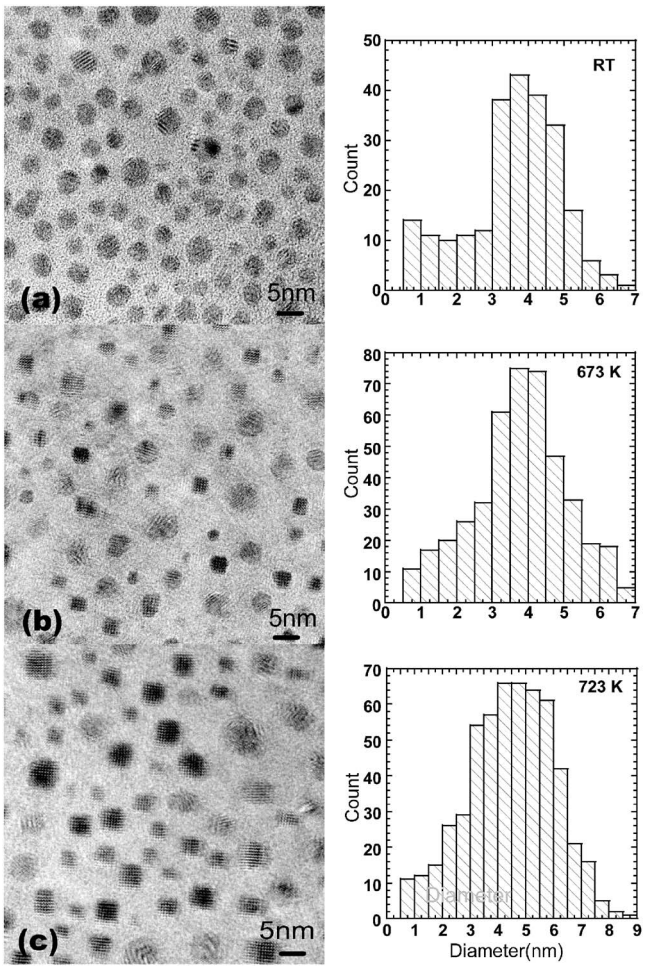


FIG. 5. The HREM images of Ag particles for the RT as-deposited (a), annealed at 673 (b), and 723 K (c), and their corresponding size distribution histgrams of Ag particles.

After annealing, the icosahedron Ag particle becomes an epitaxial truncated pyramid with four Ag (111) sidefacets, as shown in Fig. 7. For simplicity, we assume the volume $V$ of the particle remains the same. This is justified because the particle sizes only increase slightly as we discussed above.

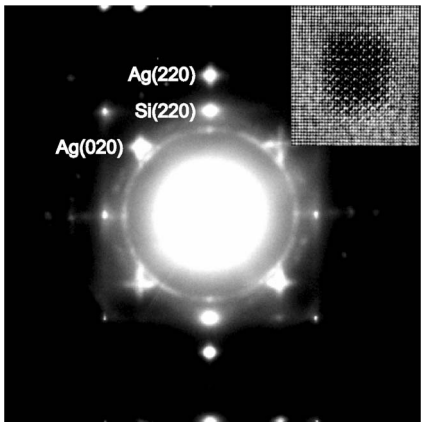


FIG. 6. A typical electron diffraction pattern of the sample annealed at 723 K. The inset is a typical epitaxial Ag nanocrystal.

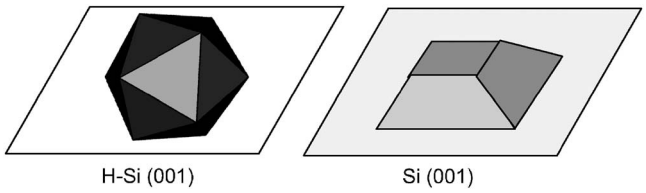


FIG. 7. A Ag icosahedron with a volume $V$ on H-Si (001). After annealing, the icosahedron transforms into a truncated pyramid.

The surface energy of the truncated pyramid-shaped particle is given as

$$E_{fcc}^{1} = \left(\frac{3V}{9.25}\right)^{2/3}\gamma_{Ag(001)} + 8.4\left(\frac{3V}{9.25}\right)^{2/3}\gamma_{Ag(111)} + 5.8\left(\frac{3V}{9.25}\right)^{2/3}(\gamma_I' - \gamma_S'), \quad (3)$$

where the first term in Eq. (3) is the top Ag (001) surface energy of the truncated pyramid, the second term is the surface energy of the side Ag (111) facets, $V$ is the volume, $\gamma_I'$ is the interfacial energy after annealing, and $\gamma_S'$ is the surface energy of H-Si(001) after annealing. We also assume that the height of the truncated pyramid is equal to the edge length of the top base.[31]

Because the lattice mismatch between Ag (001) and Si (001) is only 0.3%, we ignore the strain energy in the fcc particle, which is small compared to the surface energy. Also we neglect the difference in edge energy and cohesive energy between the icosahedron and the fcc truncated pyramid. Then the total free energy difference in the *Systeme International* (SI) unit can be expressed as

$$\Delta E = E_{fcc}^{1} - E_{Ic}^{1} - E_{Ic}^{2} = 2.5V^{2/3} - 2.8\times 10^{8}V - (2.7\beta' - 0.3\beta)V^{2/3}, \quad (4)$$

here $\beta'$ and $\beta$ are the adhesion energy between Ag and the substrate after annealing and Ag-H-Si, respectively. The adhesion energy is related to the pair-wise interaction of the involved atoms at the interface. The Dupré's relation $\gamma_I = \gamma_1 + \gamma_2 - \beta$ has been used in the above calculation. Also the following material parameters and relations are used: for Ag, the shear modulus $\mu = 4.612\times 10^{10}$ N/m$^2$, the poison ratio $\nu = 0.755$,[32] the strain in the icosahedron $\varepsilon_I = 0.0615$,[30] $\gamma_{Ag(111)} = 1.12$ J/m$^2$, $\gamma_{Ag(001)} = 1.20$ J/m$^2$; for an icosahedron, the volume $V = \frac{5}{12}(3+\sqrt{5})a^3$.

There are two extreme scenarios for the interface and substrate surface energies after annealing. The first case is that H desorbs completely after annealing. According to the first principles linearized augmented plane wave calculations, the binding energy of Ag-H-Si and Ag-Si is 0.089 and 1.61 eV/Ag atom,[25] then, substituting $\beta'$ with 1.74 J/m$^2$ and $\beta$ with 0.10 J/m$^2$, Eq. (4) becomes

$$\Delta E = -2.2V^{2/3} - 2.8\times 10^{8}V. \quad (5)$$

Therefore, in case that H completely desorbs from the Ag-Si interface, $\Delta E$ is always negative, indicating an energy gain after the structural transition due to the hydrogen desorption and the change in substrate surface and interface energy. A

similar argument also applies for a transition from decahedron to fcc.

The other extreme scenario is that H remains at the Ag-H-Si interface. In this case, the interface and surface energies are unchanged and Eq. (4) becomes

$$\Delta E = 2.26V^{2/3} - 2.8 \times 10^8 V. \quad (6)$$

In this case, if the volume of Ag particles is smaller than 527 $nm^3$ ($\sim$8 nm in diameter), $\Delta E$ is positive, suggesting that the transition from MTPs to fcc truncated pyramid nanocrystals is not energetic favorable for small particles.

The above discussion shows that the adhesion energy is critical to the stabilization or destablization of MTPs. In case of Ag on H-Si, the presence of H at the Ag/Si interface after RT deposition is supported by multiple experimental evidences,[33,34] and Ag increasingly replaces H upon annealing.[35,36] Without silver on the surface, hydrogen desorption from H-Si (001) starts at about 643 K for the dihydride phase and 733 K for the monohydride phase with desorption peaks at 698 and 813 K, respectively.[37,38] Depending on solution used in the etch, the H-Si (001) surface can be primarily either monohydride or dihydride terminated. In our experiment, a $NH_4F$ final etch produces surfaces with lower oxygen and carbon contamination levels in comparison to the surfaces obtained with the traditional HF or buffered HF etch.[39] The $NH_4F$-treated Si (001) is predominantly dihydride terminated with the $1 \times 1$ order. Annealing at 723 K in our experiment is significantly higher than the dihydride desorption peak at 698 K, thus, H desorption from the Ag and Si interface is expected. The fact that most small MTPs transforming to fcc truncated pyramids also strongly suggests H desorption from the interface and that the change in interface energy is a strong driving force for the transition as we shown.

To transform a MTP to a fcc crystal it is necessary to eliminate the multiply twinned boundaries in the MTP and change the particle shape. Atomic diffusion assisted transformation is an appealing transition mechanism. Large atomic diffusion can occur with or without particle melting. Small particles have lower melting temperatures than their bulk counterparts.[40,41] The variation of melting temperature with particle size can be expressed as[42]

$$T - T_M = -\frac{4T_M}{\rho_s LD}[\gamma_S - \gamma_L(\rho_S/\rho_L)^{2/3}], \quad (7)$$

where $T$ is the melting temperature of the particle, $T_M$ is the melting temperature of bulk silver, $L$ is the latent heat of fusion of bulk silver, $\rho$ is the mass density of the particle, $\gamma$ is the surface tension, the subscripts $S$ and $L$ represent the solid and liquid phase of the particle at the melting point $T$, and $D$ is the diameter of the particle. It is assumed in Eq. (6) that the melting is homogeneous and the particle is spherical during the melting process. Substituting numerical values for the thermodynamic quantities of bulk silver,[43] i.e., $T_M = 1234$ K, $\rho_S = 9.82 \times 10^3$ kg/$m^3$, $\rho_L = 9.33 \times 10^3$ kg/$m^3$, $L = 1.11 \times 10^5$ J/kg, $\gamma_S = 1.2$ J/$m^2$, and $\gamma_L = 0.895$ J/$m^2$, we have melting temperatures 614 and 820 K for particles with 2 and 3 nm in diameter, respectively. This indicates that silver particles smaller than 2 nm in diameter might melt homogeneously during the annealing, but larger particles most likely do not melt completely. At the annealing temperatures of $T > \sim 700$ K, the bulk diffusion length of Ag in Ag is at least several atomic spacings. The atoms at the surface are lower coordinated and weaker bonded than internal atoms, thus surface diffusion is even larger. Both the transition mechanism and the role of size-dependent melting in particle transformation are interesting issues, which deserve further investigation.

## IV. CONCLUSION

We have studied the role of substrate on the structure and transition of nanometer-sized metal particles for the case of Ag on silicon surfaces. We found that the nanometer-sized Ag particles adopt multiply twinned structures upon nucleation on H-Si (001) at room temperature, in contrast to the Ag particles of similar sizes on H-Si (111) surfaces, which assume the fcc crystal structure. Upon annealing, the Ag MTPs transform to fcc truncated pyramidal shaped nanocrystals. The driving forces for the transition are the strain energy of the MTPs and possible H desorption at the particle-substrate interface. By developing an energetic model, we show that with hydrogen at the Ag-H-Si interface, the transition from MTPs to fcc truncated pyramid nanocrystals is not energetically favorable when the volume of Ag particles is less than a critical size. In contrast, the transition from MTPs to nanocrystals is always favored if hydrogen desorbs completely from the interface.

## AKNOWLEDGMENTS

This work was supported by DOE Grant No. DEFG02-01ER45923, and was carried out in the Center for Microanalysis of Materials, University of Illinois, which is partially supported by the U.S. Department of Energy under Grant No. DEFG02-91-ER45439. The authors acknowledge the valuable discussion with Professor John H Weaver.

[1] V. A. Shchukin and D. Bimberg, Rev. Mod. Phys. **71**, 1125 (1999).
[2] J. G. Allpress and J. V. Sanders, Surf. Sci. **7**, 1 (1967).
[3] A. K. Green, E. Bauer, R. L. Peck, and J. Dancy, Krist. Tech. **5**, 345 (1970).
[4] S. Ino, J. Phys. Soc. Jpn. **27**, 941 (1969).
[5] L. D. Marks, Rep. Prog. Phys. **57**, 603 (1994).
[6] H. Haberland, *Clusters of Atoms and Molecules*, Springer Series in *Chemical Physics* Vols. 52 and 57 (Springer, Berlin, 1994).
[7] Z. L. Wang, J. Phys. Chem. B **104**, 1153 (2000).
[8] P. L. Hansen, J. B. Wagner, S. Helveg, J. R. Rostrup-Nielsen, B. S. Clausen, and H. Topsoe, Science **295**, 2053 (2002).

[9] B. Pauwels, G. Van Tendeloo, W. Bouwen, L. T. Kuhn, P. Lievens, H. Lei, and M. Hou, Phys. Rev. B **62**, 10383 (2000).
[10] D. J. Smith, A. K Petford-Long, L. R. Wallwnberg, and J. O. Bovin, Science **233**, 872 (1986).
[11] S. Iijima and T. Ichihashi, Phys. Rev. Lett. **56**, 616 (1986).
[12] B. D. Hall, D. Ugarte, D. Reinhard, and R. Monot, J. Chem. Phys. **103** 2384 (1995).
[13] M. J. Yacaman, J. A. Ascencio, H. B. Liu, and J. Gardea-Torresdey, J. Vac. Sci. Technol. B **19**, 1091 (2001).
[14] M. Hanbucken, M. Futamoto, and J. A. Venables, Surf. Sci. **147**, 433 (1984).
[15] X. F. Lin, K. J. Wan, and J. Nogami, Phys. Rev. B **47**, 13491 (1993).
[16] D. E. Starr, J. T. Ranney, J. H. Larsen, J. E. Musgrove, and C. T. Campbell, Phys. Rev. Lett. **87**, 106102 (2001), and references therein.
[17] J. C. Glueckstein, M. M. R. Evans, and J. Nogami, Phys. Rev. B **54**, R11066 (1996).
[18] B. Q. Li and J. M. Zuo, Surf. Sci. **520**, 7 (2002).
[19] B. Q. Li and J. M. Zuo, J. Appl. Phys. **94**, 743 (2003).
[20] M. T. Marshall, M. L. McDonald, X. Tong, M. Yeadon, and J. M. Gibson, Rev. Sci. Instrum. **69**, 440 (1998).
[21] J. M. Zuo, M. Gao, J. Tao, B. Q. Li, R. D Twesten, and I. Petrov, Microsc. Res. Tech. **64**, 347 (2004).
[22] A. K. Green, J. Dancy, and E. Bauer, Microsc. Res. Tech. **7**, 159 (1970).
[23] M. Gillet, Surf. Sci. **67**, 139 (1977).
[24] D. W. Pashley, Am. J. Optom. Physiol. Opt. **14**, 327 (1965).
[25] J. K. Bording, B. Q. Li, Y. F. Shi, and J. M. Zuo, Phys. Rev. Lett. **90**, 226104 (2003).
[26] F. Buatier de Mongeot, W. Zhu, A. Molle, R. Buzio, C. Boragno, U. Valbusa, E. G. Wang, and Z. Zhang, Phys. Rev. Lett. **91**, 016102 (2003).
[27] D. Reinhard, B. D. Hall, D. Ugarte, and R. Monot, Phys. Rev. B **55**, 7868 (1997).
[28] D. Winau, H. Itoh, A. K. Schmid, and T. Ichinokawa, Surf. Sci. **303**, 139 (1994).
[29] T. Tanikawa, I. Matsuda, T. Nagao, and S. Hasegawa, Surf. Sci. **493**, 389 (2001).
[30] A. Howie and L. D. Marks, Philos. Mag. A **49**, 95 (1984).
[31] The ratio of height to the edge length of the top base may vary depending on the interface energy. Our calculation shows that the selection of the ratio being 1 sets a lower limit for the energy gain in the particle transition.
[32] *CRC Handbook of Chemistry and Physics*, 85th ed., edited by David R. Lide (CRC Press, Cleveland, 2004).
[33] M. Sakurai, C. Thirstrup, and M. Aono, Phys. Rev. B **62**, 16167 (2000).
[34] A. Arranz, J. F. Sanchez-Royo, J. Avila, V. Perez-Dieste, P. Dumas, and M. C. Asensio, Phys. Rev. B **65**, 195410 (2002).
[35] K. Fukutani, H. Iwai, Y. Murata, and H. Yamashita, Phys. Rev. B **59**, 13020 (1999).
[36] M. Naitoh, A. Watanabe, and S. Nishigasi, Surf. Sci. **357**, 140 (1996).
[37] M. Suemitsu, H. Nakazawa, and N. Miyamoto, Appl. Surf. Sci. **82/83**, 449 (1994).
[38] S. M. Gates, R. R. Kuntz, and C. M. Greenlief, Surf. Sci. **207**, 364 (1989).
[39] M. R. Houston and R. Maboudian, J. Appl. Phys. **78**, 3801 (1995).
[40] M. Takagi, J. Phys. Soc. Jpn. **9**, 359 (1954).
[41] G. Bertsch, Science **277**, 1619 (1997).
[42] P. Pawlow, Z. Phys. C **65**, 1 (1909).
[43] T. Castro, R. Reifenberger, E. Choi, and R. P. Andres, Phys. Rev. B **42**, 8548 (1990).